

Supporting Information

**Construction of an Exonuclease III-propelled Integrated DNzyme
Amplifier for Highly Efficient MicroRNA Detection and Intracellular
Imaging with Ultralow Background**

*Yangjie Zhou[‡], Shanshan Yu[‡], Jinhua Shang, Yingying Chen, Qing Wang, Xiaoqing Liu and Fuan
Wang**

College of Chemistry and Molecular Sciences, Wuhan University, Wuhan, P. R. China

* To whom correspondence should be addressed. E-mail: fuanwang@whu.edu.cn.

[‡] These authors contributed equally.

Supporting Information

Table of Contents

Table S1. DNA sequence of the cascade DNzyme amplifier.....	S3
Table S2. Comparison of different Exo-III strategies for microRNA detection.....	S4
Figure S1. Validation of the cascade DNzyme amplifier.....	S5
Figure S2. Comparison of CSA and SSA systems.....	S6
Figure S3. Optimization of HP-Dz for miR-21 assay.....	S7
Figure S4. Optimization of Exo-III for miR-21 assay.....	S8
Figure S5. Optimization of Exo-III incubation condition.....	S9
Figure S6. Fluorescence miR-21 assay under short Exo-III incubation time.....	S10
Figure S7. Optimization of HP-G4 amplifier.....	S11
Figure S8. Colorimetric transduction of HP-G4 amplifier.....	S12
Figure S9. Stability of CSA machine in different matrix samples.....	S13
Figure S10. Stability of CSA machine in serum.....	S14
Figure S11. Stability of CSA machine in cell lysate.....	S15
Figure S12. Demonstration of the invasion pathway of Exo-III to living cells.....	S16
Figure S13. Effect of Exo-III on DNzyme biocatalysis.....	S17
Figure S14. Time-dependent miR-21 imaging in MCF-7 cells.....	S18
Figure S15. Feasibility of miR-21 imaging in MCF-7 cells.....	S19
References	S20

Supporting Information

Table S1. DNA sequences used for the cascade DNase amplification

No.	Sequence (5'→3')
HP-DNAzyme (HP-Dz)	CAT CAG TCG TCA TTC AGC GAT TAA CCA GGT TAC ACC CAT GTA CAG TCA AAA AAA CGC TGA ATG ACT GAT AAG CTA
HP-single (HP-S)	TCA ACA TCA GTC TGA TAA GCT AGT CAT TCA GCG ATT AAC CAG GTT ACA CCC ATG TAC AGT CAG ACT AGC TTA TCA GAC TGA
HP-G-quadruplex (HP-G4)	CAT CAG TCT GGG TAG GGC GGG TTG GGC GCC CTA CCC ATG ATA AGC TA
substrate	FAM-TGA CTG T TrAGG AAT GAC- BHQ1
as-cleaved HP-Dz	CAT CAG TCG TCA TTC AGC GAT TAA CCA GGT TAC ACC CAT GTA CAG TCA AAA AAA
miR-21	UAG CUU AUC AGA CUG AUG UUG A
anti-miR-21	TCA ACA TCA GTC TGA TAA GCT A
4-single-mutant SM1	UAG AUU AUC AGA CUG AUG UUG A
7-13-double- mutant DM1	UAG CUU UUC AGA UUG AUG UUG A
4-13-double- mutant DM2	UAG AUU AUC AGA UUG AUG UUG A
miR-429	UAA UAC UGU CUG GUA AAA CCG U
miR-141	UAC AGU AUA GAU GAU GUA CU
miR-155	UUA AUG CUA AUC GUG AUA GGG GU
miR-199a	ACA GUA GUC UGC ACA UUG GUU A
let-7a	UGA GGU AGU AGG UUG UAU AGU U

Supporting Information

Table S2. Comparison of different Exo-III strategies for microRNA detection

System	Duration (min)	Sensitivity (M)	Ref.
Single-labeled DNA probe-based aggregation-induced emission luminogens	40	1.0×10^{-12}	[1]
Exonuclease III-aided amplification on aggregation-induced emission luminogens	60	1.0×10^{-12}	[2]
DNAzyme nanomachine on AuNPs	\	1.0×10^{-10}	[3]
Triggered cascade reactions on nucleic acid templates for miR-21 assay and cell imaging	120	1.0×10^{-11}	[4]
DNAzyme-amplified DNA circuit for miR-21 assay and cell imaging	300	1.0×10^{-11}	[5]
Cascade DNAzyme amplifier for sensitive miR-21 assay and cell imaging	300	1×10^{-13}	This work

Validation of the cascade DNAzyme amplifier

The feasibility of the proposed multi-functional DNAzyme amplifier was first studied by fluorescence spectroscopy. In the presence of miR-21, the caged DNAzyme of HP-Dz was activated by Exo-III for cleaving the FAM/BHQ-1-labelled substrate and generating a high fluorescence readout. As shown in **Figure S1**, the fluorescence increased significantly after the Exo-III-assisted CSA amplifier was incubated with miR-21 (curve a), while no apparent fluorescence was observed for Exo-III-assisted CSA without miR-21 (curve b). Similarly, the Exo-III-absent CSA mixture without miR-21 (c) or with miR-21 (d) revealed no significant fluorescence change. The substrate-absent miR-21-motivated CSA system showed nearly no fluorescence with (e) or without Exo-III (f) participation. These results confirmed that the enhanced fluorescence signal was preferentially determined by the HP-Dz/miR-21 hybridization and the subsequent DNAzyme biocatalysis.

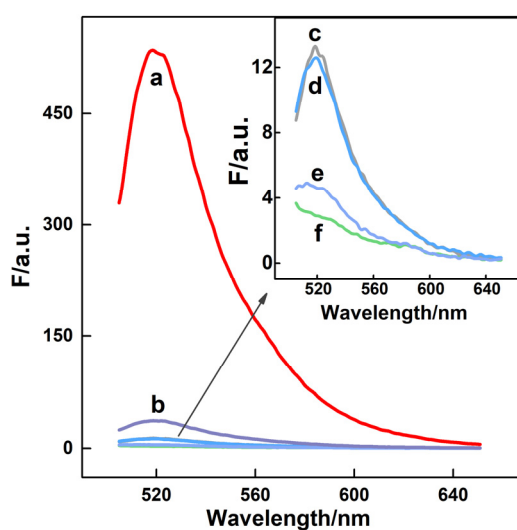


Figure S1. Fluorescence spectra responses obtained from 400 nM HP-Dz with: (a) 500 nM substrate + 60 U Exo-III and 25 nM miR-21; (b) 500 nM substrate + 60 U Exo-III; (c) 500 nM substrate; (d) 500 nM substrate + 25 nM miR-21; (e) 60 U Exo-III + 25 nM miR-21; (f) 25 nM miR-21. The cascade DNAzyme amplifier executes function in a reaction buffer (10 mM HEPES, 1 M NaCl, 100 mM MgCl₂, pH 7.2) at room temperature (25 °C) for 5 h.

Comparison of CSA and SSA systems

The CSA system proceeded from the successive Exo-III-assisted target regeneration to the subsequent DNAzyme amplification, enabling its more sensitive miR-21 assay. Accordingly, the single-staged SSA system can only activate the DNAzyme amplification without Exo-III-assisted target regeneration. Thus, the fluorescence change of SSA system cannot be observed obviously under low concentration of miR-21, and the fluorescence of 1 nM miR-21-triggered SSA system basically overlaps with the background fluorescence readout. These results indicate the prominent advantage of the Exo-III-induced target recycle and DNAzyme-catalyzed signal amplification for CSA system as compared with SSA system.

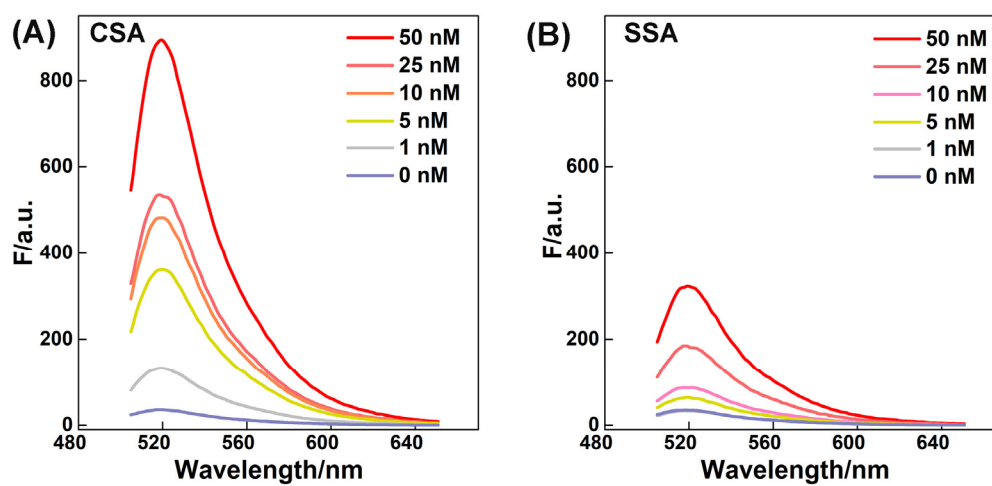


Figure S2. (A) Fluorescence responses of different miR-21 concentrations in CSA system (0 nM, 1 nM, 5 nM, 10 nM, 25 nM and 50 nM, respectively). (B) Fluorescence responses of different miR-21 concentrations in SSA system (0 nM, 1 nM, 5 nM, 10 nM, 25 nM and 50 nM, respectively).

Optimization of HP-Dz for miR-21 assay

In CSA system, the two single-stranded protruding analyte-recognition subunits in HP-Dz can hybridize with miR-21 to form a hybrid with a 3'-protruding terminus which can be identified and hydrolyzed by Exo-III. Moreover, HP-Dz maintains a stable hairpin structure without miR-21 participation because of its protruding subunits, thus an adequate amount of HP-Dz is needed to achieve target recycle. Therefore the effect of HP-Dz concentration was investigated to obtain the best analytical performance of the CSA amplifier. According to **Figure S3**, there existed weaker fluorescence intensity with lower HP-Dz concentration originating from an inefficient hybridization of HP-Dz/miR-21 duplex, while HP-Dz of higher concentration might be redundant for the whole reaction. The 400 nM HP-Dz revealed the best signal-to-background (S/B) ratio, and was then chosen in following experiments.

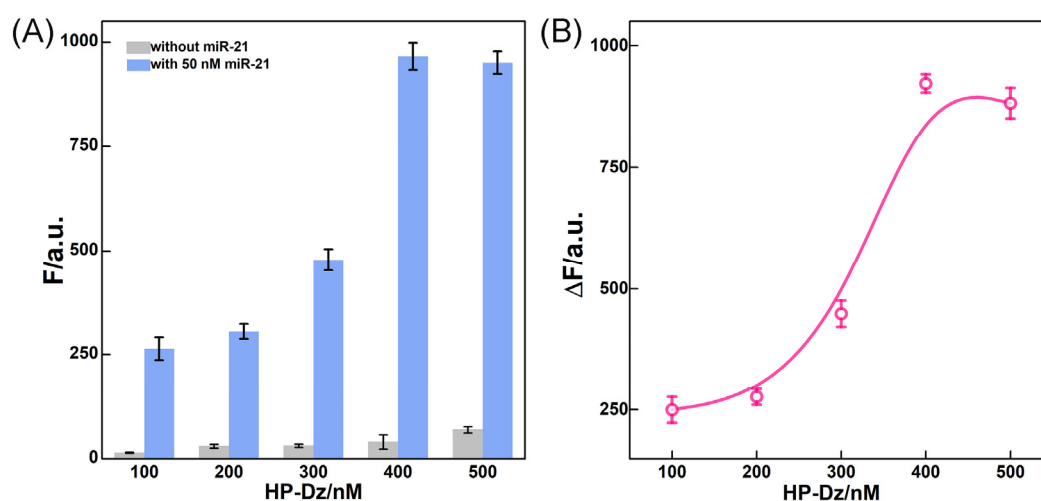


Figure S3. The effect of HP-Dz concentration was explored by fluorescence miR-21 assay in the dually amplified CSA system. (A) The histogram of fluorescence intensity of 0 nM and 50 nM miR-21 was acquired at HP-Dz ranging from 100 to 500 nM. (B) The ΔF value ($F-F_0$) was obtained at 50 nM miR-21 with different concentrations of HP-Dz as shown in **Figure S3(A)**. The amount of Exo-III, the enzymatic digestion time and reaction temperature were fixed at 60 U, 4 h and 37 °C, respectively.

Optimization of Exo-III for miR-21 assay

The performance of our multi-functional cascade DNAzyme amplifier also relies on the amount of Exo-III. The appropriate amount of Exo-III guarantees the efficient hydrolysis of HP-Dz/miR-21 duplex for regenerating miR-21 analyte and releasing DNAzyme segment. The release DNAzyme then achieves a significant fluorescence signal from the DNAzyme-catalyzed substrate cleavage. As shown in **Figure S4**, the fluorescence signal initially increased with increasing amount of Exo-III and then declined with overloaded amount of Exo-III, which was attributed to the nonspecific Exo-III digestion-generated high background signal. The signal to background ratio (S/N) reached to a maximum value at 60 U Exo-III, which was employed as the proper amount of Exo-III.

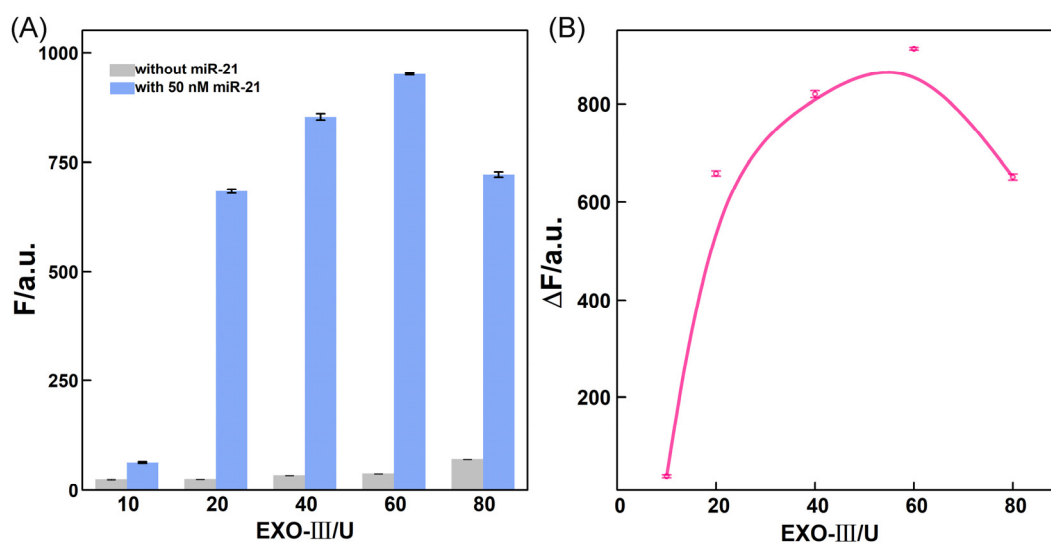


Figure S4. The effect of Exo-III amount was explored for the CSA-mediated fluorescence miR-21 assay. (A) The histogram of fluorescence intensity between 0 nM and 50 nM miR-21 was acquired at Exo-III ranging from 10 to 80 U. (B) The value of ΔF ($F - F_0$) was obtained at 50 nM miR-21 with different amounts of Exo-III.

Optimization of Exo-III incubation condition

The miR-21 regeneration and active DNAzyme acquisition depends on the digestion activity of Exo-III, which was associated with the reaction time and temperature (Figure S5). The incubation time of the DNAzyme amplifier was examined from 1 to 5 h, and the fluorescence signal reached to the saturation value when the incubation time was up to 4 h (Figures S5A and S5B). In addition, the incubation temperature was also examined. The fluorescence of the amplifier showed an increasing trend with the increasing temperature from 25 to 45 °C, and then leveled down after 37 °C (Figures S5C and S5D), which was attributed to partial enzyme inactivation at high temperature. These optimum conditions were then adapted in the subsequent experiments.

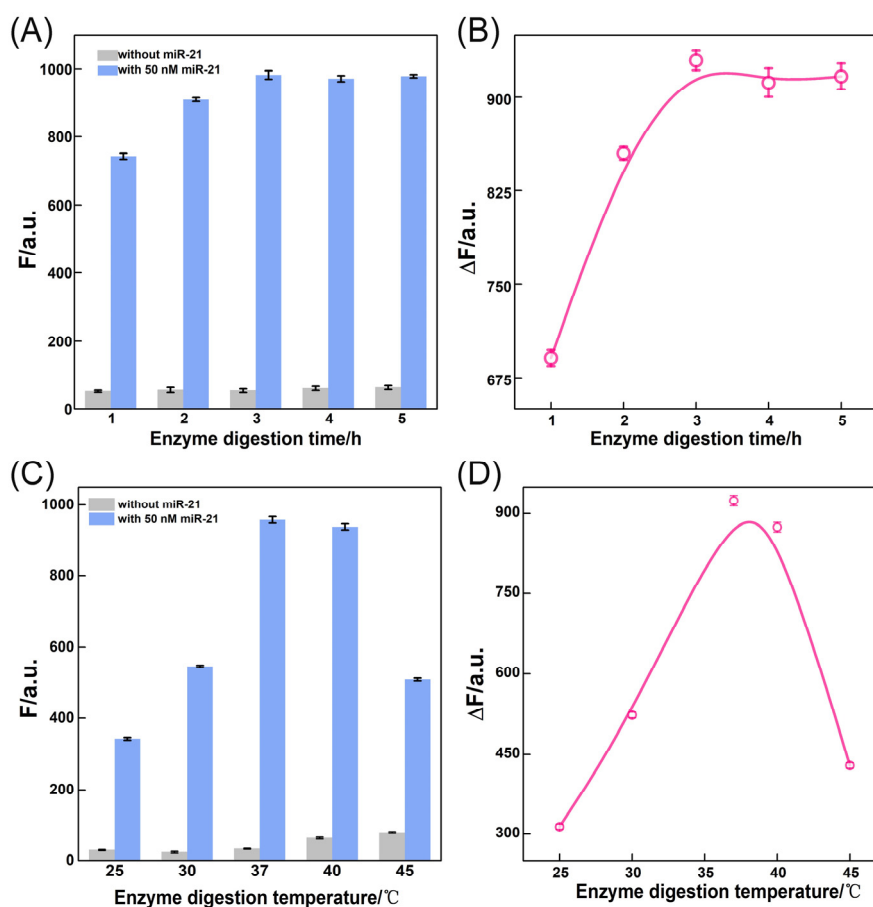


Figure S5. (A) The effect of enzymatic digestion time and (C) incubation temperature for the CSA-amplified fluorescence miR-21 assay. The value of ΔF ($F-F_0$) was obtained at 50 nM miR-21 with different digestion time (B) and incubation temperature (D) of Exo-III. The error bar represents the standard deviation of three independent measurements.

Fluorescence miR-21 assay under short Exo-III incubation time

To evaluate the multi-functional CSA system more effectively, the performance of the proposed CSA system was also explored within 10 min of Exo-III incubation. The fluorescence intensity increased gradually with increasing miR-21 concentration (**Figure S6**). In such a short time, an excellent linear correlation was acquired from the relationship between fluorescence intensity and miR-21 concentration ranging from 0.1 to 10 nM. The linear fitting equation was $F = 12.0 + 4.63 * C$ with a correlation coefficient of $R^2=0.998$. The detection of miR-21 can be achieved at 10 pM, which is substantially higher than the longer 4 h of incubation duration. It is reasonable since the signal gain of our CSA amplifier could be substantially promoted with increasing duration of Exo-III-mediated target recycling. Under the optimal experiment condition, after 4 h of incubation, the fluorescence response of our CSA machine was acquired for varied concentrations of miR-21 from 100 fM to 50 nM (**Figure 3A**). Clearly, our approach is fast response and easy operation, and the proposed multi-functional CSA system has a great potential in miR-21 detection.

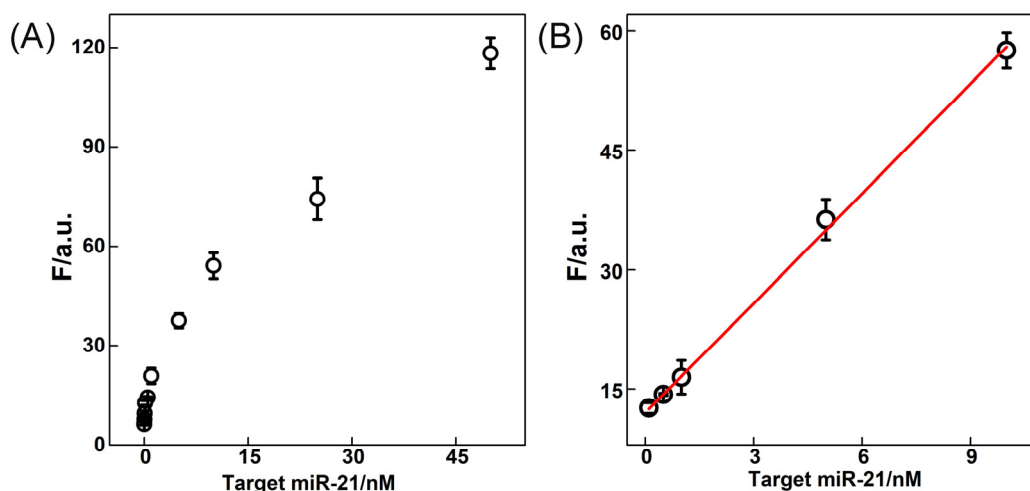


Figure S6. (A) The calibration curve of CSA system within 10 min of incubation (0 nM, 10 pM, 50 pM, 100 pM, 500 pM, 1 nM, 5 nM, 10 nM, 25 nM and 50 nM). (B) The linear fitting calibration curve between fluorescence intensity (F, at 520 nm) and miR-21 concentration. The error bar represents the standard deviation of three independent measurements.

Supporting Information

Optimization of HP-G4 amplifier

The colorimetric miR-21 assay depends on the efficient Exo-III-assisted analyte regeneration for promoting the assembly of G-quadruplex DNAzyme. Then the G-quadruplex DNAzyme can be activated spontaneously by accommodating hemin (**Figure S7A**), and the catalytic activity is dependent on the concentration of hemin, H_2O_2 and ABTS^{2-} . The best signal to noise ratio was obtained at $6\ \mu\text{M}$ of hemin (**Figure S7B**). Then the effect of H_2O_2 concentration was evaluated, and a bright green color was observed at $30\ \text{mM}$ H_2O_2 for the ABTS^{2-} catalytic oxidation reaction (**Figure S7C**). In addition, the concentration of ABTS^{2-} was also examined, and the best miR-21 assay was acquired at $6\ \text{mM}$.

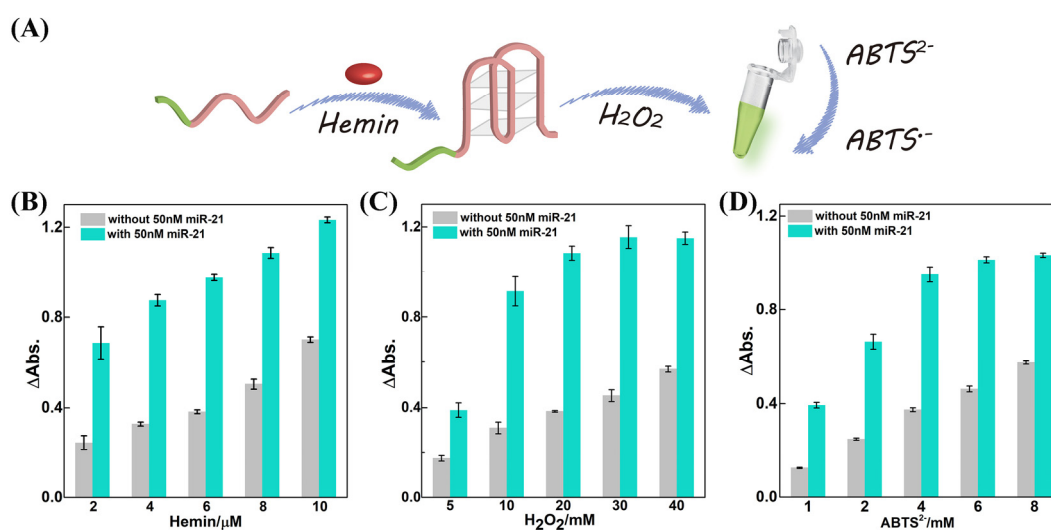


Figure S7. (A) Schematic illustration of the activated hemin/G-quadruplex-DNAzyme-catalyzed oxidation of ABTS^{2-} by H_2O_2 with color readout. Optimization of the concentration of hemin (B), H_2O_2 (C) and ABTS^{2-} (D) in the hemin/G-quadruplex HRP-mimicking DNAzyme amplifier for colorimetric assay of $50\ \text{nM}$ miR-21. Noted that the as-indicated parameter was explored under others optimal conditions. The error bars represent the standard deviation of three independent measurements.

Colorimetric transduction of HP-G4 amplifier

The proposed CSA-amplified G-quadruplex-DNAzyme could facilitate miR-21 detection with colorimetric readout. The absorbance of ABTS^{2-} (at 420 nm) was acquired by UV-vis and the corresponding photos of hemin/G-quadruplex HRP-mimicking DNAzyme-mediated color change was carried out for our CSA system. The color of CSA mixture changed gradually from colorless to deep green with increasing concentration of miR-21 analyte, and the color change of varied miR-21-triggered CSA mixture could be easily distinguished by naked eye (**Figure S8**). The result indicated the prosperity of our Exo-III-promoted target regeneration and efficient G-quadruplex-DNAzyme assembly for sensitive and label-free miR-21 assay.

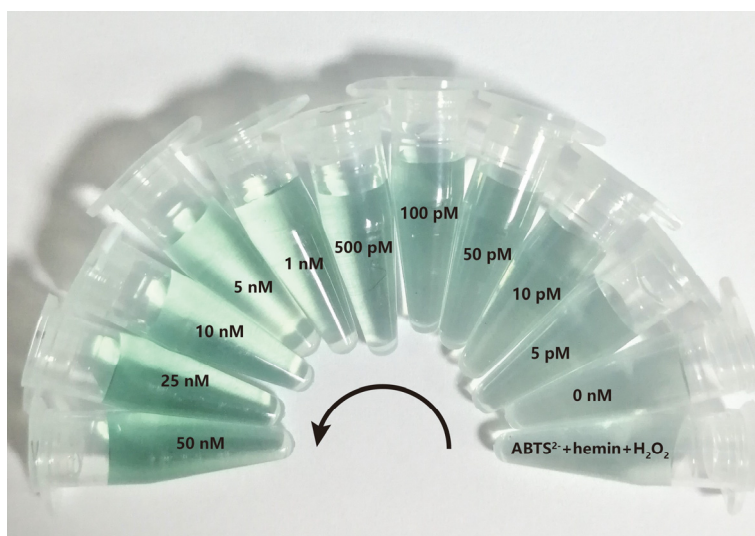


Figure. S8. CSA-mediated colorimetric analysis of miR-21 at different concentrations (0 nM, 5 pM, 10 pM, 50 pM, 100 pM, 500 pM, 1 nM, 5 nM, 10 nM, 25 nM, and 50 nM) with the naked eye observation mediated by the newly fabricated G-quadruplex-integrated HP-G4 CSA system. These photos were taken by smart phone after the implementation of the DNAzyme reaction within 5 min.

Stability of DNA machine in different matrix samples

The stability of the proposed miR-21-targeting CSA machine was evaluated by fluorescence monitoring the system incubated with different proteins and cations considering that the complex cellular environment contains plentiful of such interferents. These chosen interfering proteins are mainly associated with DNA binding, unwinding and splicing, including nicking enzyme, trypsin, DSN (duplex-specific nuclease), BSA (bovine serum albumin) and thrombin. As shown in **Figure S9(A)**, only Exo-III facilitates the amplified fluorescence transduction of miR-21 analyte while the DSN leads to a slight lower fluorescence variation. As expected, all of the other nicking enzyme, trypsin, BSA and thrombin are unable to motivate the fluorescence transduction of miR-21 analyte. This the present Exo-III-mediated CSA amplifier is robust enough to sense analyte in these enzyme-involved conditions. In addition, the possible interference of other metal ions was also explored on this CSA amplifier. The CSA amplifier system yields a tremendously amplified fluorescence transduction of miR-21 in the presence of Mg^{2+} ions, while these interfering metal ions (including Zn^{2+} , Mn^{2+} , Cu^{2+} and Ca^{2+}) obtained ultralow fluorescence variation which is comparable with the background signal (**Figure S9(B)**). It is interpretable since the DNAzyme of CSA machine relies on only Mg^{2+} ions cofactors. Also, the pH effect was also explored on the CSA amplifier. Considering the biocompatible pH environment of biological samples, the CSA-amplified miR-21 assay was carried out in different pH environments ranging from slight acid pH (pH=6.5) to basic pH (pH=8.0). As shown in **Figure S9(C)**, the CSA system exhibited a similar fluorescence transduction of miR-21 at these different pH environments. Only a slightly decreased fluorescence variation is observed for pH 8.0, which is might attributed to the inadequate Exo-III and DNAzyme biocatalysis at this basic environment. All of these mentioned interfering experimental results indicated that the CSA strategy is robust enough for ultrasensitive bioassay in potential complicated biological samples.

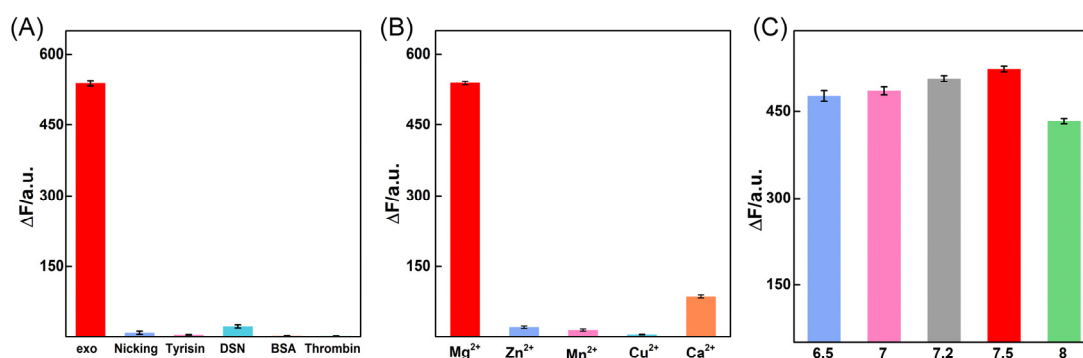


Figure S9. Fluorescence monitoring the CSA-amplified detection of miR-21 (at 520 nm) upon their incubation with different proteins (A), metal ions (B) and pH stimuli (C). The ΔF value was obtained from 25 nM miR-21-triggered multi-functional CSA system. The error bars represent the standard deviation of three independent measurements.

Stability of DNA machine in serum

It was reported that miR-21 was overexpressed in many types of cancer cells, especially breast cancer. There exists enormous interest in monitoring the expression of miR-21 in living cells, thus the complexity of biological conditions must be considered, such as human serum. The stability of our multi-functional CSA system was firstly examined in 5% and 10% healthy human serums for 5 h. The fluorescence recovery in 5% and 10% human serum samples has a good agreement with the serum-free sensing environment upon analyzing miR-21 (**Figure S10**), indicating that miR-21 could be monitored without obvious interference in real biological sample and an acceptable accuracy of the dual amplification nanomachine for target identification in complex biological fluids.

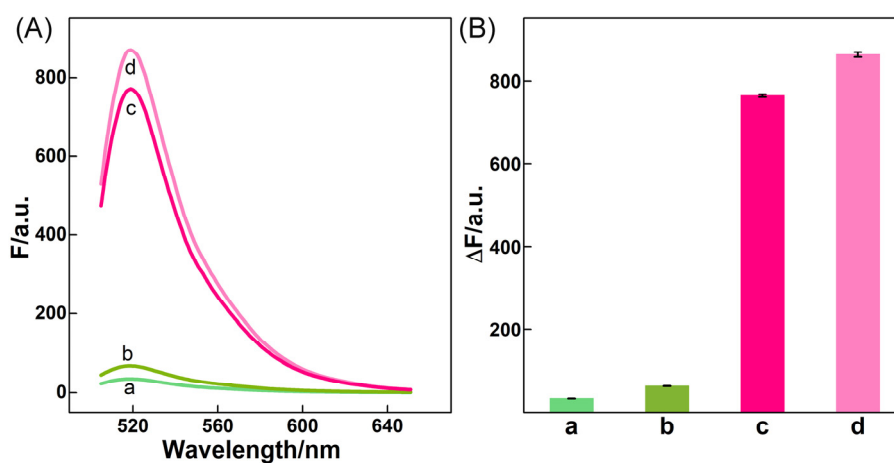


Figure S10. The stability of multi-functional cascade DNAzyme amplifier in diluted serums: (a) 5% serum, (b) 10% serum, (c) 10% serum + 50 nM miR-21 and (d) 5% serum + 50 nM miR-21. The error bars represent the standard deviation of three independent measurements.

Stability of DNA machine in cell lysate

To investigate the stability of the proposed DNA machine, we further examined the miR-21 assay in 5% and 10% MRC-5 cell lysate for 5 h incubation. As shown in **Figure S11**, without miR-21, the CSA amplifier showed a similar fluorescence variation in 5% cell lysate (c) and 10% cell lysate (e) as compared with that in reaction buffer (a). In the presence of miR-21, the fluorescence variation of our autonomous multi-functional CSA amplifier decreased slightly in 5% cell lysate (d) and 10% cell lysate (f) as compared with that in reaction buffer (b). These results suggested that our CSA system revealed excellent resistance to false signal transduction in complex biological environments.

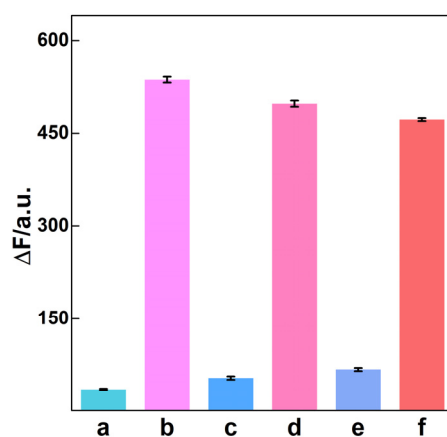


Figure S11. Fluorescence monitoring (at 520 nm) the stability of our multi-functional CSA system in (a) reaction buffer, (b) reaction buffer + 25 nM miR-21, (c) 5% MRC-5 cells lysate, (d) 5% MRC-5 cells lysate + 25 nM miR-21 (e) 10% MRC-5 cells lysate, and (f) 10% MRC-5 cells lysate + 25 nM miR-21. The error bars represent the standard deviation of three independent measurements.

Demonstration of the invasion pathway of Exo-III to living cells

The Exo-III was labeled with fluorescein isothiocyanate I (FITC) to investigate the invasion mechanism of Exo-III in MCF-7 cells with assistance of Lipofectamine 3000,^[6] which mediated the direct fusion of payload complex with the negatively charged cell membrane.^[7-8] Firstly, an sodium dodecyl sulfate polyacrylamide gel electrophoresis (SDS-PAGE) assay was performed to visualize Exo-III and FITC-labeled Exo-III (**Figures S12(A)** and **S12(B)**). Only the band of FITC-labeled Exo-III was restored with the appearance of a bright new band under 365 nm irradiation, confirming the successful labeling of FITC on Exo-III. Then the invasion pathway of Exo-III in living MCF-7 cells was investigated, and various endocytosis inhibitors were adopted to study the cellular uptake pathway. In particular, wortmannin, chloroquine phosphate, chlorpromazine, beta-cyclodextrin and NaN_3 were selected to inhibit micropinocytosis, intensity-body maturation, clathrin-mediated endocytosis, caveolae-mediated endocytosis and ATP-mediated energy metabolism, respectively. As shown in **Figure S12(C)**, the cellular uptake of Exo-III were seldom affected by these endocytosis-mediated inhibitors. The real-time CLSM imaging indicated that the FITC-labeled Exo-III gradually across the MCF-7 cells membrane into the cytoplasm (**Figure S12(D)**), indicating that Exo-III enters MCF-7 cells predominantly via a membrane fusion mechanism with the assistance of Lipofectamine 3000 transfection agents.

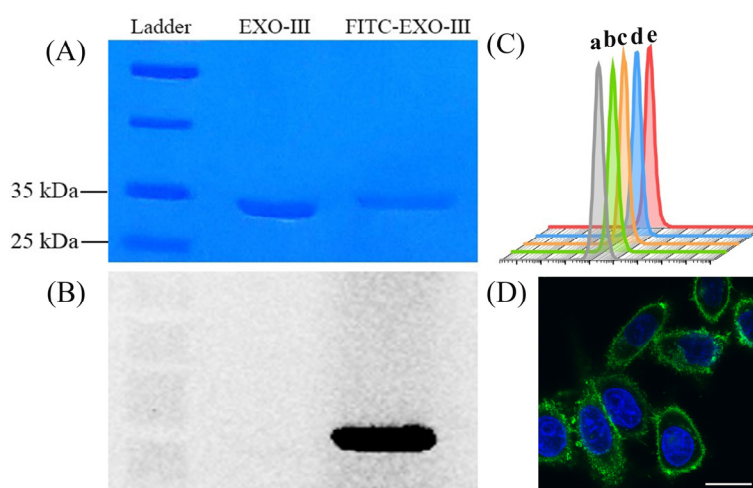


Figure S12. SDS-PAGE characterization of Exo-III and FITC-labeled Exo-III with coomassie brilliant blue solution (G250) staining (A) or 365 nm irradiation (B). (C) The corresponding flow cytometry analysis of the cellular Exo-III uptake with different endocytosis inhibitors: (a) wortmannin; (b) chloroquine phosphate; (c) chlorpromazine; (d) beta-cyclodextrin; (e) NaN_3 . (D) Real-time CLSM imaging of FITC-labeled Exo-III in MCF-7 cells. The scale bar is 20 μm .

Supporting Information

Effect of Exo-III on DNAzyme biocatalysis

The origin of fluorescence transduction needs to be explored from the hydrolysis capacity of as-achieved active DNAzyme rather than the digestion effect of Exo-III to the signal probe. Accordingly, the sequence of Exo-III-activated DNAzyme was introduced for exploring the effect of Exo-III on the as-cleaved HP-Dz probe (**Table S1**). From experimental investigation shown in **Figure S13**, the fluorescence variations of activated DNAzyme (HP-Dz fragment) and its substrate mixture showed no significant difference with and without Exo-III participation. Therefore the heating-mediated Exo-III inactivation is not the necessary step for the binding of DNAzyme with its substrate in intracellular miR-21 imaging. From the structural design proposed in **Figure 1**, Each end of the multi-functional hairpin HP-Dz was grafted with a long single-stranded DNA (containing an additional poly(A) tether), which could significantly prevent its non-specific Exo-III-mediated digestion. Meanwhile the ends of DNAzyme-cleaving substrate were respectively modified with FAM and BHQ-1, which could also prohibit the non-specific Exo-III digestion even after the substrate was specifically hybridized with the as-achieved active DNAzyme. In other words, there exists unpaired bases at both ends of the activated DNAzyme, where Exo-III could not catalyze the stepwise removal of mono-nucleotides from the protruding 3'-terminus of DNAzyme and the fluorophore-caged single-stranded DNAzyme substrate.

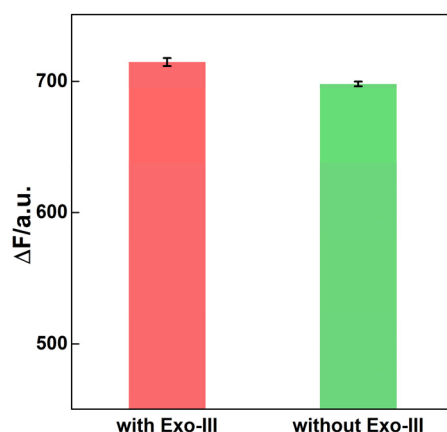


Figure S13. Fluorescence variation of the activated DNAzyme/substrate system with or without Exo-III participation ($\lambda = 520$ nm). The error bars represent the standard deviation of three paralleled experiments. The amount of DNAzyme and substrate are 400 nM and 0.5 μ M, respectively.

Time-dependent miR-21 imaging in MCF-7 cells

To further explore the CSA-mediated miR-21 imaging in live cells, the time-dependent cellular uptake of our DNAzyme machine was explored. The fluorescence signal in MCF-7 cells was gradually increased with time extension and reached to a saturation value after 4 h of incubation (Figure S14), which is therefore adopt as the optimized incubation time for the following experiments. The fast endogenous miR-21-response CSA system was thus demonstrated in living cells.

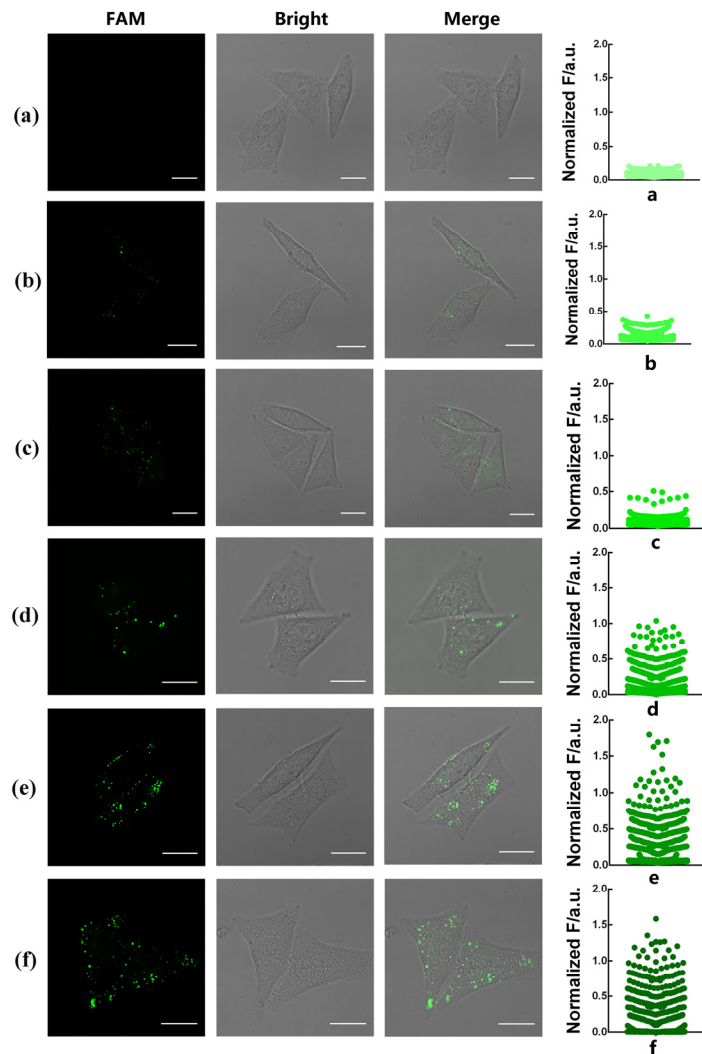


Figure S14. Real-time fluorescence imaging of miR-21 in MCF-7 cells by the multi-functional cascade DNAzyme amplifier. Scale bar = 20 μm . The green fluorescence (FAM) changes of MCF-7 cells were examined by CLSM observation and flow cytometry statistics analysis after the CSA nanomachine was incubated with MCF-7 cells for 0 h (a), 1 h (b), 2 h (c), 3 h (d), 4 h (e) and 5 h (f).

Feasibility of miR-21 imaging in MCF-7 cells

The functional integrity of the proposed multi-functional cascade DNAzyme amplifier plays a key role for intracellular miR-21 monitoring (**Figures S15A and S15B**). A much more intense green fluorescence was observed in MCF-7 cells pretreated with the integrated CSA system, but faint fluorescence signal was revealed in MCF-7 cells treated with partial CSA system. Thus only compact and integrated DNAzyme amplifier can supply extreme amplified output for intracellular miR-21. Moreover, the specificity of multi-functional CSA was further studied, and a relatively low fluorescence was obtained by treating the anti-miRNA antisense inhibitor oligonucleotide (miR-21 inhibitor), indicating that the fluorescence of living cells was ascribed to miR-21 recognition. Additionally, flow cytometry was then applied to analyze the fluorescence transduction of these systems with larger cell population. As anticipated, MCF-7 cells transfected with integrated nanomachine displayed a huge fluorescence signal shift (**Figure S15C**), which were consistent with the corresponding CLSM characterizations.

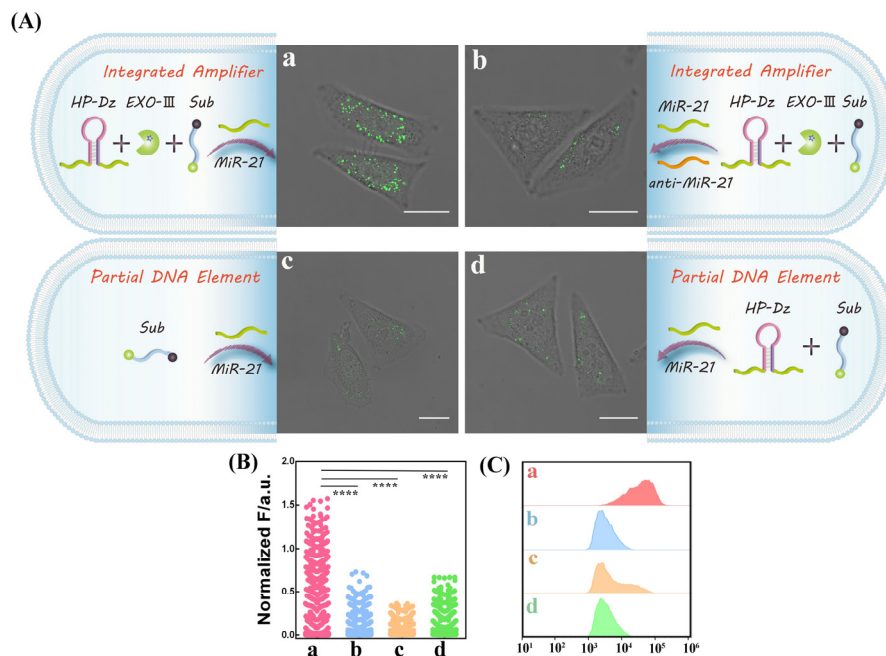


Figure S15. (A) Real-time CLSM images of MCF-7 cells treated with integrated multi-functional cascade DNAzyme amplifier (a), integrated multi-functional cascade DNAzyme amplifier + miR-21 inhibitor (500 nM) (b), partial functional DNA element (250 nM substrate) (c) and partial functional DNA element (625 nM HP-Dz + 250 nM substrate) (d) for 4 h. Scale bar = 20 μm. (B) The data statistics of CLSM and (C) the flow cytometry analysis of MCF-7 cells that were pretreated with relevant different treatments. All of the aforementioned living cells were transfected and incubated with nanoprobe at 37 °C for 4 h.

References

- (1) Min, X.; Zhuang, Y.; Zhang, Z.; Jia, Y.; Hakeem, A.; Zheng, F.; Cheng, Y.; Tang, B.; Lou, X.; Xia, F. Lab in a Tube: Sensitive Detection of MicroRNAs in Urine Samples from Bladder Cancer Patients Using a Single-Label DNA Probe with AIEgens. *ACS Appl. Mater. Interfaces*. **2015**, *7*, 16813–16818.
- (2) Min, X.; Zhang, M.; Huang, F.; Lou, X.; Xia, F. Live Cell MicroRNA Imaging Using Exonuclease III-Aided Recycling Amplification Based on Aggregation-Induced Emission Luminogens. *ACS Appl. Mater. Interfaces*. **2016**, *8*, 8998–9003.
- (3) Liu, J.; Cui, M.; Zhou, H.; Yang, W. DNAzyme based Nanomachine for *in situ* Detection of MicroRNA in Living Cells. *ACS Sens.* **2017**, *2*, 1847–1853.
- (4) Ren, K.; Zhang, Y.; Zhang, X.; Liu, Y.; Yang, M.; Ju, H. *In situ* SiRNA Assembly in Living Cells for Gene Therapy with MicroRNA Triggered Cascade Reactions Templated by Nucleic Acids. *ACS Nano*. **2018**, *12*, 10797–10806.
- (5) Wang, H.; Wang, H.; Wu, Q.; Liang, M.; Liu, X.; Wang, F. DNAzyme-Amplified DNA Circuit for Highly Accurate MicroRNA Detection and Intracellular Imaging. *Chem. Sci.* **2019**, *10*, 9597 – 9604.
- (6) Brinkley, M. A Brief Survey of Methods for Preparing Protein Conjugates with Dyes, Haptens, and Cross-Linking Reagents. *Bioconjugate Chem.* **1992**, *3*, 2-13.
- (7) Hirko, A.; Tang F.; Hughes J. Cationic Lipid Vectors for Plasmid DNA Delivery. *Current Medicinal Chemistry*. **2003**, *10*, 1185-1193.
- (8) Chesnoy, S.; Huang, L. Structure and Function of Lipid-DNA Complexes for Gene Delivery. *Annual Review of Biophysics & Biomolecular Structure*. **2000**, *29*, 27-47.